

# Detecting Flooded Locations Using SAR DATA, and Assessment of Post-Flooded Condition

**Moung-Jin Lee** Korea Environment Institute, 339-007 10F, Bidg. B, 370 Sicheong-daero, Sejong-si, Korea

## Keywords

Flooded Damage, Multi-Temporal SAR Data, GIS

The aim of this study is to detect flooded locations using SAR data and assess post-flooded conditions using a Geographic Information System (GIS) and SAR (Synthetic Aperture Radar) data images. The temporal characteristics of radar response from flooding were analyzed throughout the 2002 summer flood season. Flooded locations were identified through a change detection technique of RADARSAT SAR data images. Multiple Radarsat SAR images were acquired before, during, and after the flood inundation. From the interpretation of colour composite imagery of the multi-temporal SAR data, as well as from the temporal profiles of radar backscatter, seven types of landcover could be classified according to flooded and post-flooded recovery conditions. Landcover map of 2000.07 was divided into 7 categories: water, urban, bare ground, marsh, grassland, forest and farming. From the images, it was determined that the farming area showed flooding in 14.52km<sup>2</sup>, the forest flooded area was 3.50km<sup>2</sup>, the grassland flooded area was 1.06km<sup>2</sup>, the ground flooded area accounted for 0.09km<sup>2</sup> and the urban flooded area was 0.04km<sup>2</sup>. The actual flooded damage to the standing farming crop depends on the duration of the flood and on the subsequent recovery status. We found that image data acquired during and after a flood is needed to assess accurately flood damage to a farming area. In this study result are proved in the scientific basis for flood damage. The findings of this study will contribute to reducing the hazards of natural disasters and will increase the flexibility in the process of managing damage caused by natural disasters.

## Introduction

The Korean Peninsula has been damaged by rain storms caused by Typhoon Kai-tak in 2000, Jebi in 2001, Rusa in 2002, Maemi in 2003, and Ewiniar in 2006. In the 2000s, the rain storms caused by constant typhoons developed into floods and there has been flood damage every year. Of the natural disasters caused by floods, flood damage has the longest-lasting effects. Flood damage has a higher frequency of occurrence than any other natural disaster, creating tremendous economic losses, including immense casualties and the destruction of buildings and of fertile land.

In this study, the author utilized Synthetic Aperture Radar (SAR), a type of satellite image. The passive optical images using sunlight as energy source in satellite images are mostly affected by the conditions of the atmosphere and the weather. However, the SAR is not affected by weather conditions such as cloud, mist, rain, and smoke and fog because it is an active sensor system using the satellite itself as energy source. Also, unlike an optical satellite image, which has limitations to its capacity to obtain data, the system obtains images even at night and can provide image data taken at any time. In this context, the system has the potential to be used in disaster monitoring related to natural disaster. The SAR can take images even in the middle of flood damage, and therefore help to show the direction for the prevention of damage.

The purpose of this study is to enhance the utility of SAR as a type of satellite image in the event of flood damage. To accomplish this, the areas of actual flood damage were extracted using radar satellite images, and then the flood damage was analyzed according to the actual conditions of land use by overlapping with the land cover map.

## Methodology and Contents

### Study Area

Between August 3 and 5, 2002, there were rain storms in Yongyeon (250mm), Haeju (233mm), Kaesung (159mm), and Gusung (126mm) in Hwanghaenam Do, Hwanghaebuk Do, Pyungannam Do, and Pyunganbuk Do, North Korea. Of the areas that experienced damage caused by floods, Jelyoung, Hwanghaebuk Do is at the center of the fertile Jaeryung Plain located in the drainage basin of Jaeryung River, and serves as a trading center for agro-livestock products. In addition, Jelyoung coalfield and many factories of farm machines and implements are located around the area.

Various time series images are needed in order to identify areas of damage caused by floods. Images taken in July 15, 2002 before the flood damage and those taken in September 1, 2002 after the damage were acquired, as these were the images closest to the flood period. The images of September 1, 2002 were taken around a month after the flood caused by the rain storm, and show the augmentation of water flows of reservoirs and lakes after the completion of drainage, as well as the flood damage occurring around reservoirs and lakes. Therefore, the research area in this study was limited to around the lakes of Jelyoung area.

### Time Series Radar Satellite Image Data

The image data used in this study were from a C-band radar image system taken by DARASAT with the wavelength of 5.6cm. The images used in the research were taken in standard mode, and had a spatial resolution of about 12.5m, covering about  $110 \times 120\text{km}^2$  in a take. The research area in this study covered  $32 \times 25\text{km}$ , which included reservoirs and lakes among the whole images.

Because the SAR is an active system, there is speckle noise. To address this phenomenon, the images were first treated with Sigma Nought and a LEE Filter was applied. Sigma Nought is the degree of returning the radiation of incident microwave to the radar, indicating backscatter coefficient. It is generally expressed as data value with the unit of dB, and is considered of the incidence angle against the range of satellite in SAR images. In other words, it is considered of the effects of side-looking at the maximum. It plays an important role in the quantitative interpretation of radar image system data. LEE Filter is usually applied to radar data to preserve the high frequency characteristics, such as edge, and to eliminate high frequency noises. It smooth out the speckles characteristic to DNs.

Table 1. Using SAR Image in this study.

Date	Beam mode	Incidence angle	Dimension	Pixel size	Georeferenced Data
2002.07.15	Standard(F3)	42.6°	110*110km <sup>2</sup>	12.5m	SGF Product
2002.09.01	Standard(F6)	42.2°			

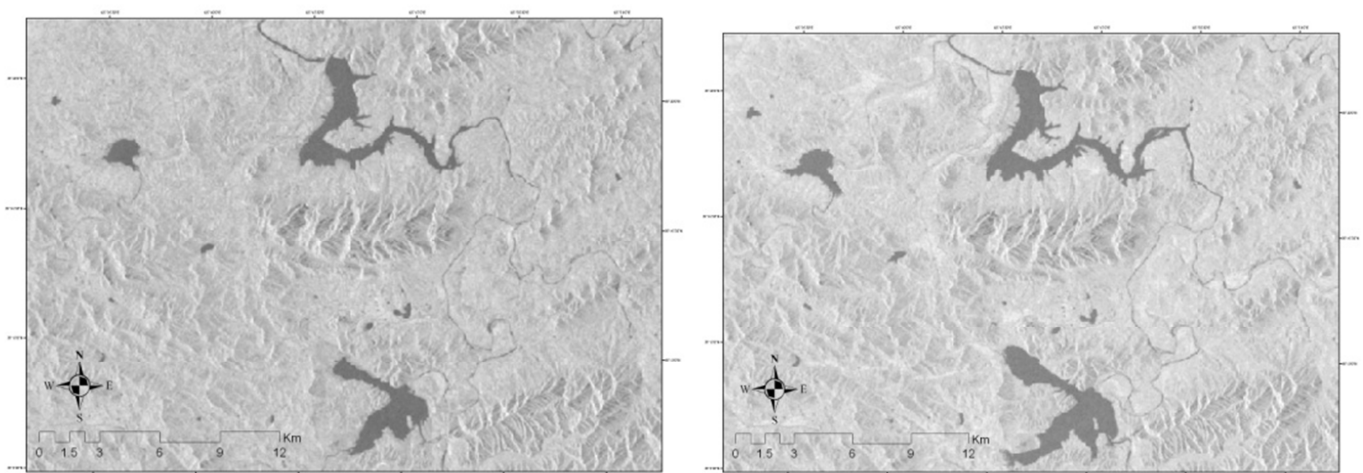


Figure 1. Study Area (2002.07.15, Before), Right : 2002.09.01, after) in Flooding occurred.

## Application of Change Detection Technique of Radar Satellite Image and Overlapping Analysis of Land Use Map

Change detection through the use of satellite images is a favorable method to detect the changes of the surface of the earth. The changes may be detected if satellite image data are acquired with time series, and the changes in the images taken at various periods can be emphasized in their pixel values according to the changes in time. The information can be made into a database, which is used to monitor the changes on the surface of the earth. Position correction of the images is most critical for change detection. Even an error of a half pixel may become serious later. Therefore, it is easier and more accurate to perform precise geometric correction for one image from the two for comparison by using digital topographic maps, and then to apply the same geometric correction points to the other one. In order for the images and land cover maps of the two periods to be in accord in the same locations, the images of SAR and land cover maps were corrected based on the landsat images taken in August 16, 1999. The ground control points that could be identified in each image were selected, coordinate transformation was produced through the points, and the other image was re-arranged according to the coordinates of the reference image.

In order to analyze the actual conditions of the damage according to land use in the areas of flood damage built through change detection technique, overlap analysis was performed with land cover maps made from the Landsat images taken in August 16, 1999.

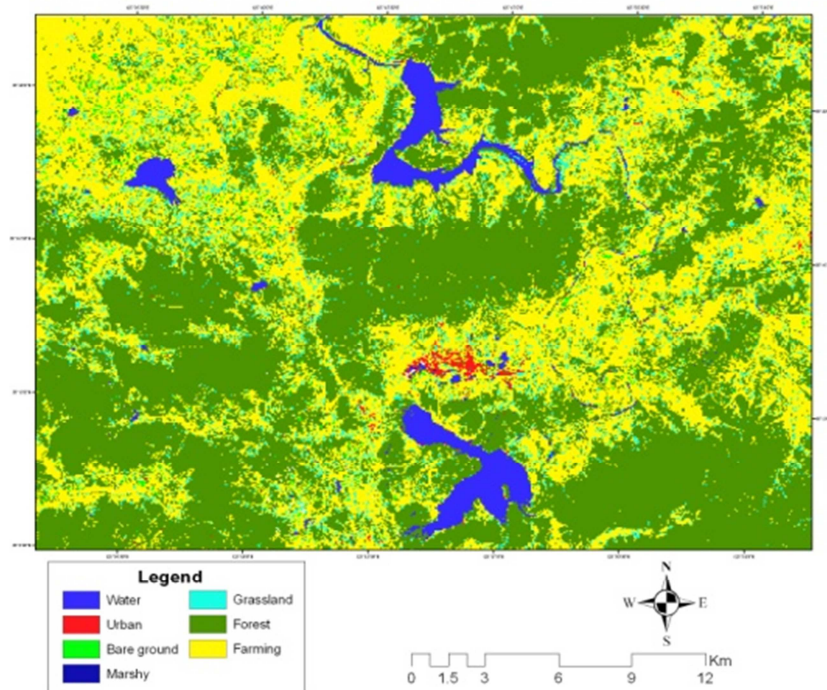


Figure 2. Landcover Map.

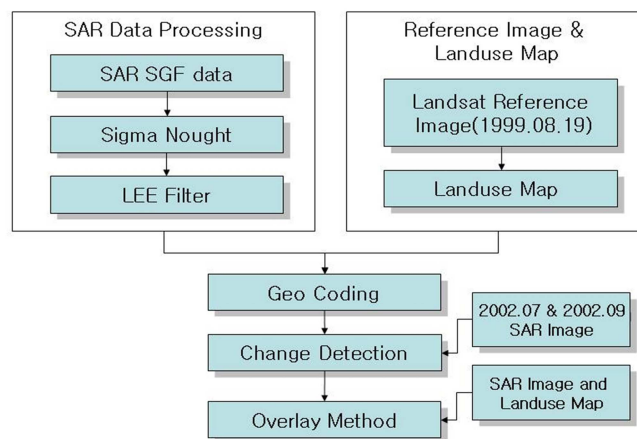
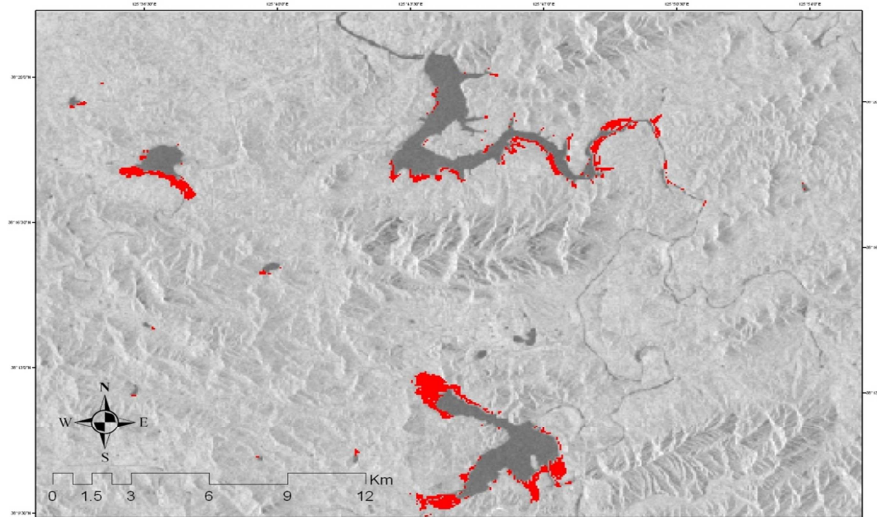


Figure 3. Process adopted by this study.



**Figure 4.** Flooded Area in result of change detection

**Table 2.** Analysis of Flooded Area.

Class	Total Dimension (km <sup>2</sup> )	Flooded Area Dimension (km <sup>2</sup> )	Flooded Area ratio (%)	Each Class Flooded ratio (%)
Water	24.87	0.00	0.10	0.00
Urban	3.15	0.04	1.34	0.20
Bare ground	7.66	0.09	1.18	0.45
Marshy	0.06	0.00	1.90	0.00
Grassland	43.31	1.06	2.45	5.30
Forest	408.28	3.50	0.86	17.95
Farming	295.68	14.42	4.88	76.10
Total	783	20.00	-	100

## Results

For this study, the flood damage studied was caused by the rain storm of August 2002, which occurred in Jelyoung. The total size of the research area was 783km<sup>2</sup>. The areas of flood damage that were analyzed through time series radar images amounted to 20km<sup>2</sup>. The rate of the size of the flooded area in the whole area studied was about 3%. Figure 4 shows the whole flooded area, which was extracted by using a change detection technique on time series radar images.

In Table 2, the three areas where there is a great deal flooded among the flooded areas were selected in order to be expanded and arranged. As seen in Table 2, areas with much flooding were located in areas with arrows (showing the directions of water system) and relatively low slope.

This phenomenon is considered to correspond with the topographical and geological logics in which flooded areas occur in the direction of a water system and then in low-slope areas. When this viewpoint is applied to the areas with flooded damage in this study, the flooded areas researched are highly likely to become habitual flooded areas.

As result, it was found that the farming area showed 14.42km<sup>2</sup> flooded, the forest flooded area was 3.50km<sup>2</sup>, the grassland flooded area was 1.06km<sup>2</sup>, the ground flooded area accounted for 0.09km<sup>2</sup> and the urban flooded area was 0.04km<sup>2</sup>

## Discussion & Conclusion

In this study, time series radar satellite images were used to extract flooded areas and to compare and analyze the actual conditions of land use. In this study results are extending and apply to another flooding area, Based on the result, the measures to enhance the utility of the radar images in the environmental sphere were examined, and policies to alleviate flooding damage through land use planning were presented. However, it cannot be said that the measures derived in this study reflect all of the possible approaches to minimizing the damage of flooding. Therefore, in order for the results derived from this study to be applied to the policy-making process in the future, it is absolutely necessary to verify the results through a field inspection, and to discuss the methods of prevention of flooding damage, including the flooding damage prediction map.

## Acknowledgments

This research was supported by Basic Science Research Program of Korea Environmental Institute (KEI) funded by the National Research Foundation of Korea (NRF) funded by the Ministry of Education (NRF-2014R1A1A1002704). ■



### Moungh-Jin Lee

Dr. Moungh-Jin Lee got his Ph.D. in remote sensing and geographic information system from Yonsei University (Department of Earth System Sciences). He is currently a research scientist in the Korea Environment Institute. Prior to joining KEI, Dr. Lee worked in the companies related to remote sensing and GIS carried out several projects in the field of environments. His research interest is the remote sensing in the natural disaster, especially the landslide and flood in the city. An estimation of natural disaster by using data mining methods such as spatial statistics and probabilistic model is also another field of interests.

E-mail: leemj@kei.re.kr

## References

- [1] Guy J P Schumanna, Jeffrey C Neala, David C Masonb, Paul D Batesa (2011) The accuracy of sequential aerial photography and SAR data for observing urban flood dynamics, a case study of the UK summer 2007 floods. *Remote Sensing of Environment* 115(10): 2536-2546
- [2] K S LEE, S I LEE (2003) Assessment of post-flooded conditions of rice fields with multi-temporal satellite SAR data. *International Journal of Remote Sensing* 24:17, 3457-3465
- [3] Pulvirentia, M Chinib, N Pierdiccaa, L Guerrieroc, P Ferrazzolic (2010) Flood monitoring using multi-temporal COSMO-SkyMed data: Image segmentation and signature interpretation. *Remote Sensing of Environment* 115(4): 990-1002
- [4] R Hostachea, P Matgena, W Wagnerb (2012) Change detection approaches for flood extent mapping: How to select the most adequate reference image from online archives?. *International Journal of Applied Earth Observation and Geoinformation* 19: 205-213
- [5] L Giustarinia, H Vernieuweb, J Verwaerenb, M Chinia, R Hostachea, P Matgena (2015) Accounting for image uncertainty in SAR-based flood mapping. *International Journal of Applied Earth Observation and Geoinformation* 34: 70-77
- [6] Stefan Schlaffera, Patrick Matgenb, Markus Hollausa, Wolfgang Wagnera (2015) Flood detection from multi-temporal SAR data using harmonic analysis and change detection. *International Journal of Applied Earth Observation and Geoinformation* 38: 15-24
- [7] Guy J-P Schumanna, Jeffrey C Neala, David C Masonb, Paul D Batesa (2011) The accuracy of sequential aerial photography and SAR data for observing urban flood dynamics, a case study of the UK summer 2007 floods. *Remote Sensing of Environment* 115(10): 2536-2546
- [8] Santiago Zazo, José-Luis Molina, Pablo Rodríguez-Gonzálvez (2015) Analysis of flood modeling through innovative geomatic methods. *Journal of Hydrology* 524: 522-537
- [9] Anthea L. Mitchella, Ian Tapleyb, Anthony K. Milnea, Mark L. Williams, Zheng-Shu Zhoud, Eric Lehmann, Peter Caccettad, Kim Lowelle, Alex Heldf (2014) C- and L-band SAR interoperability: Filling the gaps in continuous forest cover mapping in Tasmania. *Remote Sensing of Environment* 155: 58-68
- [10] Mahyat Shafapour Tehrani, Biswajeet Pradhan, Shattri Mansor, Noordin Ahmad (2015) Flood susceptibility assessment using GIS-based support vector machine model with different kernel types. *CATENA* 125: 91-101